Flexural Study of a Neutrally Buoyant Inflated Viscoelastic-Structural Member

A. K. Misra* and V. J. Modi†
University of British Columbia, Vancouver, B.C., Canada

Flexural deflection of a neutrally buoyant inflated viscoelastic cantilever is studied using the three parameter solid model. This is followed by a free vibration analysis in the presence of hydrodynamic drag and axial tension. The approximate solutions of the governing nonlinear, partial differential equation are substantiated through numerical and experimental data. The paper ends with the dynamical response analysis to surface wave excitation. The information so generated has direct relevance to the design of an underwater submarine detection system.

Nomenclature

$b_r(\xi)$ = coefficient of α^r, Eq. (27)
d = diameter
h = wall thickness
p = internal pressure
r = radius
t = time
$\tilde{t}$ = dimensionless time variable, Eq. (27)
$w(x,t)$ = flexural displacement
$w_{v.e.}(x,t)$ = viscoelastic displacement
x = axial distance of a point from the fixed end
z = transverse distance of a point from the neutral axis
A = area of cross section
A_k, B_k = constants, Eq. (36)
A_{or} = coefficients of $\Psi_r(\xi)$ in the eigenfunction expansion of the initial displacement, Eq. (29)
C_d = drag coefficient based on projected area Ld
C_m = added inertia coefficient
C_{ki} = coefficient of Φ_i in the eigenfunction expansion of $d^2\Phi_k/d\xi^2$, Eq. (37)
E = Young's modulus
E_1, E_2, ν_2 = three parameters of viscoelastic solid
F = tip load
I = moment of inertia of the cross section
$J(t)$ = creep compliance in tension
$J_s(t)$ = creep compliance in shear
K_r = normalizing multiplier, Eq. (18b)
L = length of cantilever
P = pressure parameter
R = axial force
$W(x)$ = function of x, Eq. (11)
α = damping parameter, $2C_d/\pi(C_m+1)$
β_{irs} = a constant, Eq. (30b)
γ = nondimensional viscoelastic damping coefficient, measure of energy loss in the structure
δ_{ij} = deflection at station i due to the load at station j
δ_ℓ = tip deflection
$\eta(\xi,\tau)$ = dimensionless displacement, w/d
η_c, η_s = cosine and sine components of η, Eq. (34)
η_0 = dimensionless wave amplitude
λ_i = principal stretches
μ = modulus of rigidity
μ_r = eigenvalues of a cantilever
μ_r', μ_r'' = functions of eigenvalues and pressure parameter, Eq. (19)
ξ = dimensionless distance from the fixed end, x/L
ρ, ρ_w = densities of structural material and water, respectively
σ_r = functions of μ_r, μ_r' and μ_r'', Eq. (19c)
σ_{ij} = stress tensor
τ = dimensionless time, $[EI/A\rho_w(1+C_m) \times L^4]^{1/2}t$
$\phi_0, \phi_{-1}, \phi_1$ = scalar functions of principal stretches, Eq. (3)
ω = frequency
$\Phi_i(\xi)$ = eigenvalues of a cantilever without axial force
$\Psi_i(\xi)$ = eigenfunctions of a cantilever with axial force, Eq. (18)
$\Psi_i^*(\xi)$ = eigenfunctions for the adjoint problem;

$$\int_0^l \Psi_i \Psi_j^* d\xi = \delta_{ij}$$

Presented as Paper 74-139 at the AIAA 12th Aerospace Sciences Meeting, Washington, D.C., January 30-February 1, 1974; submitted April 17, 1974; revision received May 9, 1975. The investigation reported here was supported by the Defense Research Board of Canada, Grant 9550-38.

Index category: Structural Dynamic Analysis.

*Graduate Research Fellow, Department of Mechanical Engineering.

†Professor, Department of Mechanical Engineering. Member AIAA.

I. Introduction

In recent years foldable or inflatable structures have gained much prominence because of their compactness and light weight. Inflated cylindrical structures have been suggested for fuselage construction while inflated plates may be used for the wings of re-entry gliders and the control surfaces of satellites. As regards the underwater applications, neutrally buoyant inflated structures have been proposed for a variety of missions like submarine detection, oceanographic survey, lifting surfaces of hydrofoil type vehicles, etc. Consider, for example, the problem of patrolling of submarines. It is currently undertaken in various ways, such as: a) long range patrol aircraft equipped with radar which can detect the surfaced or snorkeling subs; b) "turnstiles" placed across the various gateways to the major ocean basins; c) fixed site or towed sonar system; and d) sonobuoys providing platforms for hydrophones and telemetering system.

Theoretically, at least three or four hydrophones are needed to locate an object in two or three dimensions, respectively. It has been established that the efficiency of this operation can be improved considerably by using an array of inflatable tubes.

These possible applications have led to the investigations aimed at better understanding the structural behavior of an inflatable member. The review of the available literature suggests that the interest in the field is of relatively recent origin. This is further emphasized by the fact that the available design oriented information is rather limited. Leonard, Brooks and McComb[1] calculated the buckling and collapse loads for inflated cantilever structures. It was observed that the local buckling starts when the compressive stress due to a bending moment just cancels the tensile stress due to the internal pressure, and the structure collapses when the resisting "plastic hinge" moment is exceeded by the moment caused by the load. Stein and Hedgepeth[2] considered an inflated circular cylindrical tube carrying a constant moment and obtained a relation between the beam curvature and the moment. Comer and Levy[3] studied the deflection of an inflated elastic cylindrical cantilever beam when the load exceeded the buckling value and obtained the tip deflection and maximum stress. The relation between the shearing stiffness and inflation pressure, accounting for the beam edge effect, has been determined by Topping.[4] These investigators observed that the flexural stiffness is essentially independent of the internal pressure. But Douglas,[5] using the finite theory of elasticity, has shown how the structural stiffness of an inflated cylindrical cantilever is influenced by the large deformations which occur during inflation. The analysis covers a rather wide range of inflation pressures leading to a change in diameter as high as 400%. It was observed that the inflation pressure has a linear relationship with the stretch in diameter only in the early stages of inflation (up to about 40% stretch in diameter) and is independent of the dimensionless scaling factor β characterizing the deformation. On the dynamical side, the available literature is conspicuously scarce. Landweber[6,7] and Warnock[8] investigated the dynamics of an elastic cylinder in an incompressible, inviscid fluid to determine the apparent mass effects in the absence of hydrodynamic drag. The vibration of an inflated cylindrical cantilever has been studied by Douglas.[9] But the hydrodynamic forces are absent as the structure is oscillating in air. The general case of a dissipative system with axial tension due to inflation pressure remains virtually untouched.

The precise knowledge of stiffness and dynamical characteristics of these inflatable members, which are generally made of plastic materials like polyethylene, mylar, etc. or sandwich materials formed out of them, is a prerequisite to any attempt at a structural design using them. This paper aims at taking a small step in that direction. In the beginning, flexural deflection of a neutrally buoyant inflated viscoelastic cantilever is studied using the three parameter solid model in conjunction with the correspondence principle. The analytical procedure is substantiated through an experimental program employing several polyethylene models. The importance of this approach cannot be overemphasized as it represents a simple procedure, well-suited for a design office, for assessing time dependent stiffness of such structural members. This is followed by a free vibration analysis of the cantilevered member in the presence of hydrodynamic drag and axial tension, the latter arising due to inflation pressure. The effect of added inertia is also accounted for. The governing nonlinear, partial differential equation, judiciously nondimensionalized to make the damping parameter independent of the geometrical dimensions of the beam is studied using two analytical procedures: a) mode approximation in conjunction with the Krylov and Bogoliubov method, which yields essentially the same results as the first-order perturbation; b) more precise second-order perturbation technique.

The validity of the approximate methods is established by comparing the results, over a range of system parameters, with numerical and experimental data. The paper ends with the dynamical response analysis of a viscoelastic, inflated cantilever to surface wave excitation.

II. Analytical Development

A. Statics

Consider a neutrally buoyant inflated cylindrical cantilever (Fig. 1a) of initial length L_0, diameter d_0, wall thickness h_0, and internal pressure p. Let the initial dimensions of the cylinder and those at any instant during inflation be related by the principal stretches,

$$L=\lambda_1 L_0,\ d(=2r)=\lambda_2 d_0,\ h=\lambda_3 h_0 \tag{1}$$

Assumption of incompressibility of the material leads to

$$\lambda_1\lambda_2\lambda_3=1 \tag{2}$$

As shown by Douglas[5] using the finite theory of elasticity, the principal stresses are given by

$$\sigma_{11}=\phi_0+\phi_1\lambda_1^2+\phi_{-1}\lambda_1^{-2}=pr/2h \tag{3a}$$

$$\sigma_{22}=\phi_0+\phi_1\lambda_2^2+\phi_{-1}\lambda_2^{-2}=pr/h \tag{3b}$$

$$\sigma_{33}=\phi_0+\phi_1\lambda_3^2+\phi_{-1}\lambda_3^{-2}=O(p) \tag{3c}$$

where ϕ_i are scalar functions of the diagonal stretch matrix. Since σ_{33} is small compared to σ_{11} or σ_{22} (the ratio being of the order of h/r), it may be neglected. With this approximation, one obtains from Eqs. (2) and (3)

$$(\lambda_1^2\lambda_2^4-1)(\phi_1-\lambda_1^2\phi_{-1})=2(\lambda_1^4\lambda_2^2-1)(\phi_1-\lambda_2^2\phi_{-1}) \tag{4}$$

For a material obeying the Mooney-Rivlin constitutive equations, ϕ_1 and ϕ_{-1} are constants:

$$\phi_1=\mu(\tfrac{1}{2}+\beta);\ \phi_{-1}=-\mu(\tfrac{1}{2}-\beta) \tag{5}$$

where μ is the shear modulus of the undeformed material, and β is a dimensionless scaling factor.

It has been found that inflation is independent of β for moderate stretches (up to about 40% increase in diameter).[5] Since in the present case inflation lies within this range an arbitrary β (including $\beta=0$) may be assumed to obtain a relation between p and λ_i. Taking $\beta=0$, $\phi_1=\mu/2$ and $\phi_{-1}=-\mu/2$. With this, Eq. (4) yields

$$\lambda_1^2=1 \tag{6a}$$

and Eq. (2) reduces to

$$\lambda_2\lambda_3=1 \tag{6b}$$

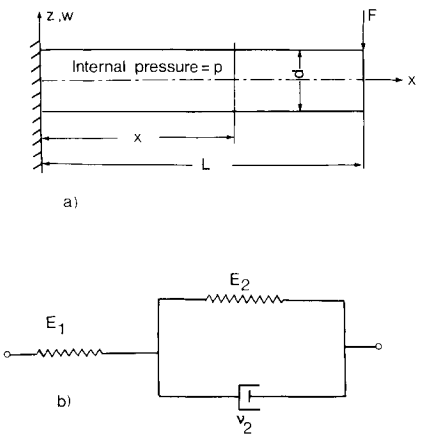

Fig. 1 a) Geometry of the system; b) Three parameter viscoelastic solid.

Previous relations together with Eq. (3) lead to

$$\lambda_2 = (1 - pr_0/\mu h_0)^{-1/4} \simeq 1 + pr_0/4\mu h_0$$

since $pr_0/4\mu h_0$ is small in the present case. Thus

$$r = r_0(1 + pr_0/4\mu h_0) \tag{7}$$

In the actual practice, a change in length is small compared to the changes in the diameter and thickness. Hence $\lambda_1 = 1$, i.e., $\beta = 0$, represents a good approximation in evaluating changes in the dimensions due to inflation.

Equation (7) suggests that the variation in radius is proportional to the internal pressure. To account for the time dependent properties of the material, the equation can be modified to

$$r(t) = r_0[1 + pr_0 J_s(t)/4h_0]$$

where $J_s(t)$ is the creep compliance in shear and p the step pressure applied at $t = 0$. The radius after a long time is thus given by

$$r_f = r_0[1 + pr_0 J_s(\infty)/4h_0] \tag{8a}$$

with the final thickness as

$$h_f = h_0[1 - pr_0 J_s(\infty)/4h_0] \tag{8b}$$

The cantilever beam is now allowed to undergo bending deformations. It will be assumed that there are no wrinkles in the structure. Wrinkles appear as soon as the stress at any point becomes compressive. So the internal pressure should be sufficient to make the resultant stress tensile everywhere. The elastic solution must be obtained before the viscoelastic one, which is then realized by the correspondence principle. The resultant stress on an element with coordinates (x,z) is given by superposing the stresses due to bending and inflation pressure, i.e.,

$$\sigma_{11} = pr_f/2h_f + F(L-x)z/I \tag{9}$$

where F is the load and I is the moment of inertia of the cross-section

$$I = \pi r_f^3 h_f$$

The curvature is approximately given by

$$d^2w/dx^2 = -F(L-x)/EI \tag{10}$$

Integrating and using the boundary conditions at $x = 0$, lead to

$$w(x) = -(FL^3/6EI)[(x/L)^2(3 - x/L)] = W(x)/E \tag{11}$$

If the stress level is not too high, the materials used for inflatable structures behave like a linear viscoelastic solid. In that case a three parameter solid (Fig. 1b) can represent the material behavior fairly well since the long time creep is very small. But this is not true if the stress level is high. However even in that case the creep in the initial stages can be represented fairly well by the aforementioned model.

Applying the correspondence principle,

$$\bar{w}_{v.e.}(x,s) = \bar{w}(x,s)E/s\bar{E}(s) \tag{12}$$

where $\bar{w}_{v.e}(x,s)$, $\bar{w}(x,s)$ and $\bar{E}(s)$ are the Laplace transforms of the viscoelastic solution, elastic solution, and the relaxation modulus of the material, respectively. For a 3-parameter solid,

$$s\bar{E}(s) = E_1(E_2 + \nu_2 s)/(E_1 + E_2 + \nu_2 s)$$

where E_1, E_2, and ν_2 are the 3 parameters defining the material behavior. Thus,

$$\bar{w}_{v.e.}(x,s) = W(x)(E_1 + E_2 + \nu_2 s)/E_1(E_2 + \nu_2 s)s$$

and on inverting

$$w_{v.e.}(x,t) = W(x)[(1/E_1) + (1/E_2)\{1 - \exp(-E_2 t/\nu_2)\}]$$
$$= W(x)J(t) \tag{13}$$

where $W(x)$ is given by Eq. (11).

B. Dynamics

Free vibration of an inflated elastic cylindrical cantilever under water

Neglecting the effects of rotary inertia and shear deformation, the equation of motion of an elastic cylinder (Fig. 1a) in water is given by

$$EI\partial^4 w/\partial x^4 + A\rho_w(1 + C_m)\partial^2 w/\partial t^2 - R\partial^2 w/\partial x^2$$
$$+ \tfrac{1}{2}C_d d\rho_w \partial w/\partial t\,|\partial w/\partial t| = 0 \tag{14}$$

where added inertia and drag coefficients C_m and C_d, respectively, somewhat vary with the size of the cylinder, period of oscillation and maximum velocity.[10] (The coefficient C_m in Ref. 10 corresponds to the total intertia force, not the added inertia force.) However, for simplicity, they are assumed to remain essentially constant in the present analysis. This appears logical in light of the fact that as the period parameter is increased the total inertia coefficient first falls from the theoretical value to a minimum and then gradually increases to a value of 2.5. On the other hand, C_d shows exactly the opposite behavior. Hence, in general the sum of the two forces deviates relatively less from the theoretical value.

Defining

$$\eta = w/d, \qquad \xi = x/L$$
$$\tau = [EI/A\rho_w(1 + C_m)L^4]^{1/2}t, \quad P = RL^2/EI \tag{15}$$

Equation (14) can be nondimensionalized as

$$\partial^4\eta/\partial\xi^4 - P\partial^2\eta/\partial\xi^2 + \partial^2\eta/\partial\tau^2 + \alpha\partial\eta/\partial\tau\,|\partial\eta/\partial\tau| = 0 \tag{16a}$$

where

$$\alpha = 2C_d/\pi(C_m + 1) \tag{16b}$$

It may be noticed that the damping parameter α is independent of the geometrical dimensions of the cylinder. The boundary conditions are given by

$$\eta(0,\tau) = \partial\eta(0,\tau)/\partial\xi = \partial^2\eta(1,\tau)/\partial\xi^2$$
$$= \partial^3\eta(1,\tau)/\partial\xi^3 = 0 \tag{16c}$$

Let the initial conditions be

$$\eta(\xi,0) = A_0(\xi) \text{ and } \partial\eta(\xi,0)/\partial\tau = 0 \tag{16d}$$

This is a nonlinear partial differential equation with no known exact solution. Hence one is forced to resort to approximate or numerical analysis. Two distinct approaches have been attempted. Since the equation is moderately nonlinear and the displacement-time relation is usually more important than the displacement variation along the length, it may be assumed that the mode shape does not deviate substantially from the linear case. This approximation yields a nonlinear ordinary differential equation which can be solved by the Krylov-Bogoliubov method. An alternate approach

would be the perturbation technique which yields relatively more accurate results but leads to complicated expressions.

Mode Approximation Method

The nondimensionalized equation of motion in the absence of hydrodynamic drag is given by

$$\partial^4\eta/\partial\xi^4 - P\partial^2\eta/\partial\xi^2 + \partial^2\eta/\partial\tau^2 = 0 \tag{17}$$

The previous equation can easily be solved by the separation of variables[11] and the solution can be shown to be

$$\eta(\xi,\tau) = \sum_{r=1}^{\infty} \Psi_r(\xi) f_r(\tau) \tag{18a}$$

where

$$\Psi_r(\xi) = K_r[(\cosh\mu_r''\xi - \cos\mu_r'\xi) - \sigma_r\{\sinh\mu_r''\xi - (\mu_r''/\mu_r')\sin\mu_r'\xi\}] \tag{18b}$$

and

$$f_r(\tau) = A_r\cos\mu_r^2\tau + B_r\sin\mu_r^2\tau \tag{18c}$$

Here

$$\mu_r''^2 = (\mu_r^4 + P^2/4)^{1/2} + P/2 \tag{19a}$$

$$\mu_r'^2 = (\mu_r^4 + P^2/4)^{1/2} - P/2 \tag{19b}$$

$$\sigma_r = [\cosh\mu_r'' + (\mu_r'^2/\mu_r''^2)\cos\mu_r'] / [\sinh\mu_r'' + (\mu_r'/\mu_r'')\sin\mu_r'] \tag{19c}$$

and μ_r are the roots of the frequency equation

$$P^2 + 2\mu^4(1+\cosh\mu''\cos\mu') - \mu^2 P\sinh\mu''\sin\mu' = 0 \tag{20}$$

The coefficients K_r are so chosen as to normalize $\Psi_r(\xi)$, i.e.,

$$\int_0^1 \Psi_r^2(\xi)\,d\xi = (1/4)[\Psi_r^2(1) + (P/\mu_r^4)\{d\Psi_r(1)/d\xi\}^2] = 1 \tag{21a}$$

From Eq. (18b), with the help of Eq. (20) one obtains

$$\Psi_r^2(1) = K_r^2[(\mu_r'^2 + \mu_r''^2)^2/\mu_r'^3\mu_r''^3][(\mu_r'^3\sinh\mu_r'' + \mu_r''^3\sin\mu_r')/(\mu_r''\sinh\mu_r'' + \mu_r'\sin\mu_r')] \tag{21b}$$

and

$$[d\Psi_r(1)/d\xi]^2 = K_r^2[(\mu_r'^2 + \mu_r''^2)^4/4\mu_r'^4\mu_r''^4] \times [\{(\mu_r'^2 - \mu_r''^2) + \mu_r'\mu_r''\sinh\mu_r''\sin\mu_r'\}/(\mu_r''\sinh\mu_r'' + \mu_r'\sin\mu_r')]^2 \tag{21c}$$

Substitution of the previous relations in Eq. (21a) yields K_r. Then A_r and B_r may be evaluated from the initial conditions. The objective here is to employ these modes in the analysis of the nonlinear Eq. (16).

If the oscillation comprises of a single mode close to the one given by Eq. (18b)

$$\partial^4\eta/\partial\xi^4 - P\partial^2\eta/\partial\xi^2 \simeq \mu^4\eta$$

Equation (16a) now yields a nonlinear differential equation

$$\partial^2\eta/\partial\tau^2 + \mu^4\eta + \alpha(\partial\eta/\partial\tau)\,|\partial\eta/\partial\tau| = 0 \tag{22}$$

As the nonlinearity is not too strong ($\alpha \simeq 0.35$), the Krylov-Bogoliubov method[12] may be used to yield the solution of the form,

$$\eta = A(\xi,\tau)\cos[\mu^2\tau + \theta(\tau)] \tag{23}$$

where $A(\xi,\tau)$ and $\theta(\tau)$ are slowly varying functions of τ and can be obtained from the following averaging relations:

$$\dot{A} = -(\alpha/\mu^4)(\mu^2/2\pi) \int_0^{2\pi} \mu^4 A\sin\zeta\,|A\sin\zeta|\sin\zeta\,d\zeta = -4\alpha\mu^2A^2/3\pi \tag{24a}$$

and

$$\dot{\theta} = -(\alpha/\mu^4)(\mu^2/2\pi A)\int_0^{2\pi} \mu^4 A\sin\zeta\,|A\sin\zeta|\cos\zeta\,d\zeta = 0 \tag{24b}$$

Therefore, the solution becomes

$$\eta = [A(\xi,0)/(1+4\alpha\mu^2A(\xi,0)\tau/3\pi)]\cos[\mu^2\tau + \theta(0)] \tag{25}$$

Equation (25) shows a decay in the amplitude of the motion with time in the presence of hydrodynamic drag. On the other hand, the frequency of oscillation remains unaffected, at least up to the first-order approximation.

Perturbation Method

The governing Eq. (16a) may be rewritten as

$$\partial^4\eta/\partial\xi^4 - P\partial^2\eta/\partial\xi^2 + \partial^2\eta/\partial\tau^2 \pm \alpha(\partial\eta/\partial\tau)^2 = 0 \tag{16a'}$$

where the appropriate sign is chosen so as to oppose the motion. It is sufficient to solve Eq. (16a') either for positive or negative sign for half a cycle, as the solution for the other half may be obtained simply by reversing the sign of α with the new initial conditions.

The solution for the negative sign is sought in the form

$$\eta(\xi,\tau) = \eta_0(\xi,\tau) + \alpha\eta_1(\xi,\tau) + \alpha^2\eta_2(\xi,\tau) + \ldots. \tag{26}$$

A new time variable $\tilde{t}$ is defined by

$$\tilde{t} = \tau[1 + \alpha b_1 + \alpha^2 b_2 + \ldots.] \tag{27}$$

Since the period of oscillation may vary slowly across the length, b_1 and b_2 are slowly varying functions of ξ. With Eqs. (26) and (27), Eq. (16a') becomes

$$\partial^4(\eta_0 + \alpha\eta_1 + \alpha^2\eta_2 + \ldots.)/\partial\xi^4 - P\partial^2(\eta_0 + \alpha\eta_1 + \alpha^2\eta_2 + \ldots.)/\partial\xi^2 + [1 + \alpha b_1 + \alpha^2 b_2 + \ldots.]^2 \times [\partial^2(\eta_0 + \alpha\eta_1 + \alpha^2\eta_2 + \ldots.)/\partial\tilde{t}^2 - \alpha\{\partial(\eta_0 + \alpha\eta_1 + \alpha^2\eta_2 + \ldots.)/\partial\tilde{t}\}^2] = 0$$

Equating the coefficients of the different powers of α to zero separately, one obtains

$$\alpha^0:\ \partial^4\eta_0/\partial\xi^4 - P\partial^2\eta_0/\partial\xi^2 + \partial^2\eta_0/\partial\tilde{t}^2 = 0 \tag{28a}$$

$$\alpha^1:\ \partial^4\eta_1/\partial\xi^4 - P\partial^2\eta_1/\partial\xi^2 + \partial^2\eta_1/\partial\tilde{t}^2 = -2b_1(\xi)(\partial^2\eta_0/\partial\tilde{t}^2) + (\partial\eta_0/\partial\tilde{t})^2 \tag{28b}$$

$$\alpha^2:\ \partial^2\eta_2/\partial\xi^4 - P\partial^2\eta_2/\partial\xi^2 + \partial^2\eta_2/\partial\tilde{t}^2 = -[2b_2(\xi) + b_1^2(\xi)](\partial^2\eta_0/\partial\tilde{t}^2)$$

$$+2b_1(\xi)\left[(\partial\eta_0/\partial\tilde{t})^2-\partial^2\eta_1/\partial\tilde{t}^2\right]+2(\partial\eta_0/\partial\tilde{t})(\partial\eta_1/\partial\tilde{t}) \tag{28c}$$

etc.

The objective is to solve this system of equations such that all η_i's confirm to the boundary conditions (16c) with initial conditions (16d) satisfied by η_0 alone, while zero initial conditions are met by other η_i's.

The solution to Eq. (28a) can be written as

$$\eta_0(\xi,\tilde{t})=\sum_{r=1}^{\infty}A_{0r}\Psi_r(\xi)\cos\mu_r^2\tilde{t} \tag{29a}$$

where $\Psi_r(\xi)$ and μ_r are defined by Eqs. (18b) and (20), respectively, and

$$A_{0r}=\int_0^1 A_0(\xi)\Psi_r^*(\xi)d\xi \tag{29b}$$

With this, the solution to Eq. (28b) is

$$\eta_1(\xi,\tilde{t})=-\tfrac{1}{2}\sum_{i=1}^{\infty}\sum_{r=1}^{\infty}\sum_{s=1}^{\infty}\beta_{irs}\mu_r^2\mu_s^2A_{0r}A_{0s}\Psi_i(\xi)$$
$$\times\left[\{\cos\mu_i^2\tilde{t}-\cos(\mu_r^2-\mu_s^2)\tilde{t}\}/\{\mu_i^4-(\mu_r^2-\mu_s^2)^2\}\right.$$
$$\left.-\{\cos\mu_i^2\tilde{t}-\cos(\mu_r^2+\mu_s^2)\tilde{t}\}/\{\mu_i^4-(\mu_r^2+\mu_s^2)^2\}\right] \tag{30a}$$

where

$$\beta_{irs}=\int_0^1\Psi_i^*(\xi)\Psi_r(\xi)\Psi_s(\xi)d\xi \tag{30b}$$

and to avoid secular terms

$$b_1(\xi)=0 \tag{30c}$$

The solution to Eq. (28c) can similarly be obtained.

For the positive sign in Eq. (16a′) the solution is similar except that the sign of η_1 is different. The complete solution is obtained by using the two solutions alternately and determining the amplitude at the start of each half cycle.

Now certain particular intial conditions may be considered.

Case 1: Let the initial conditions be

$$\eta(\xi,0)=A\Psi_1(\xi),\quad \partial\eta(\xi,0)/\partial\tau=0$$

Here $A_{01}=A$ and $A_{0i}=0$ $(i=2,3,\ldots\infty)$ Noting that $(\mu_1/\mu_2)^4$, $(\mu_1/\mu_3)^4$ etc. are small compared to 1,

$$\eta(\xi,\tilde{t})\simeq A\Psi_1(\xi)\left[\cos\mu_1^2\tilde{t}+\alpha\beta_{111}A\{(\tfrac{1}{2})-(\tfrac{2}{3})\cos\mu_1^2\tilde{t}\right.$$
$$+(1/6)\cos2\mu_1^2\tilde{t}\}-\alpha^2\beta_{111}^2A^2\{(2/3)+(8/9)\cos\mu_1^2\tilde{t}$$
$$\left.+(2/9)\cos2\mu_1^2\tilde{t}\}\right] \tag{31a}$$

where

$$\tilde{t}=\tau[1-\alpha^2\beta_{111}^2A^2/6] \tag{31b}$$

The cylinder comes to rest again when

$$\tau=\tau_h=\pi/\mu_1^2(1-\alpha^2\beta_{111}^2A^2/6)$$

Correspondingly, $\eta(\xi,\tau_h)=\bar{A}$(say). The solution can now be obtained for the next half cycle by replacing $-\alpha$ by $+\alpha$ and A by $\bar{A}$. Case 2: Let the initial displacement correspond to the second mode,

$$\text{i.e., } \eta(\xi,0)=A\Psi_2(\xi),\quad \partial\eta(\xi,0)/\partial\tau=0$$

Following a procedure similar to that in Case 1, the first-order perturbation solution is obtained to be

$$\eta(\xi,\tau)\simeq\Psi_2(\xi)\left[A\cos\mu_2^2\tilde{t}-(\alpha/2)\beta_{222}A^2\{(4/3)\cos\mu_2^2\tilde{t}\right.$$
$$\left.-1-(\tfrac{1}{3})\cos2\mu_2^2\tilde{t}\}\right]-(\alpha/2)A^2\Psi_1(\xi)\beta_{112}(\mu_2/\mu_1)^4$$
$$\times(\cos\mu_1^2\tilde{t}-1)$$

Note that the coefficient of $\Psi_2(\xi)$ as represented by the square bracket diminishes with time, hence the motion tends to reduce to that given by the first case. As any set of initial conditions may be written as a linear combination of various mode shapes and since the first few modes are likely to be the most dominating, the analysis may be confined to the first two modes only.

Forced vibration of an inflated cylindrical cantilever with velocity square damping

Consider an inflated cylindrical cantilever oscillating under the influence of ocean waves. It is assumed that the motion of a water particle due to the waves can be approximated to a sinusoidal function. The steady-state response of a viscoelastic system can be studied either using the correspondence principle in conjunction with an elastic solution or by including equivalent dissipative terms representing energy loss due to viscoelasticity. For a three parameter solid the complex modulus can be represented as

$$E^*(\omega)=E_1(E_2+i\nu_2\omega)/[E_1+(E_2+i\nu_2\omega)]$$
$$=E_1[1-E_1/(E_1+E_2+i\nu_2\omega)]$$

In the present case $(E_1+E_2)/\nu_2\omega$ was found to be of the O(1/100) and hence can be neglected, thus reducing the expression to

$$E^*(\omega)=E_1[1+i\omega(E_1/\nu_2\omega^2)]=E_1[1+i\omega\gamma(\omega)]$$

Adopting this latter procedure, the nondimensionalized equation can be written as

$$(1+\gamma\partial/\partial\tau)\partial^4\eta/\partial\xi^4-P\partial^2\eta/\partial\xi^2+\partial^2(\eta+\eta_w)/\partial\tau^2$$
$$+\alpha\partial(\eta+\eta_w)/\partial\tau\,|\partial(\eta+\eta_w)/\partial\tau|=0 \tag{32}$$

where η is the nondimensionalized displacement of any point on the cantilever with respect to its root, γ is the measure of energy loss in the viscoelastic structure dependent on frequency, and η_w is the nondimensionalized wave displacement given by

$$\eta_w=\eta_0\cos\omega\tau \tag{33}$$

Here τ is defined in Eq. (15) with E replaced by the instantaneous modulus of elasticity E_1.

The system has both external as well as parametric excitations, thus presenting a possibility of parametric instability. However, in the actual system, this has never been observed. From practical considerations, it is the knowledge of the steady-state response which is more essential to isolate the actual signal received by the hydrophones at the tip of the cantilever. Hence the efforts are concentrated on finding such solutions.

In general the solution will contain all the harmonics of ω. However, for simplicity, only the fundamental term will be considered, i.e., the solution is of the form

$$\eta=\eta_c(\xi)\cos\omega\tau+\eta_s(\xi)\sin\omega\tau \tag{34}$$

Substitution of Eqs. (33) and (34) in Eq. (32) leads to

$$(1+\gamma\frac{\partial}{\partial\tau})[(d^4\eta_c/d\xi^4)\cos\omega\tau+(d^4\eta_s/d\xi^4)\sin\omega\tau]$$
$$-P[(d^2\eta_c/d\xi^2)\cos\omega\tau+(d^2\eta_s/d\xi^2)\sin\omega\tau]$$
$$-\omega^2[(\eta_0+\eta_c)\cos\omega\tau+\eta_s\sin\omega\tau]+\alpha\omega^2[-(\eta_c+\eta_0)\sin\omega\tau$$
$$+\eta_s\cos\omega\tau]\,|-(\eta_c+\eta_0)\sin\omega\tau+\eta_s\cos\omega\tau|=0$$

Multiplication by $\cos\omega\tau$ and $\sin\omega\tau$ separately and integration over one period gives

$$d^4(\eta_c+\gamma\omega\eta_s)/d\xi^4-Pd^2\eta_c/d\xi^2-\omega^2(\eta_c+\eta_0)$$
$$+8\alpha\omega^2\eta_s[(\eta_c+\eta_0)^2+\eta_s^2]^{1/2}/3\pi=0 \tag{35a}$$
$$d^4(-\gamma\omega\eta_c+\eta_s)/d\xi^4-Pd^2\eta_s/d\xi^2-\omega^2\eta_s$$
$$-8\alpha\omega^2[\eta_c+\eta_0][(\eta_c+\eta_0)^2+\eta_s^2]^{1/2}/3\pi=0 \tag{35b}$$

The quantities η_c and η_s can be represented as

$$\eta_c(\xi)=\sum_{k=1}^{\infty}A_k\Phi_k(\xi) \tag{36a}$$
$$\eta_s(\xi)=\sum_{k=1}^{\infty}B_k\Phi_k(\xi) \tag{36b}$$

where $\Phi_k(\xi)$'s are the eigenfunctions of a cantilever (without axial tension) and are given by Eq. (18b) after putting $K_r=1$, $P=0$. Since $d^2\Phi_k/d\xi^2$ can be represented as an infinite sum of $\Phi_i(\xi)$,

$$d^2\eta_c/d\xi^2=\sum_{k=1}^{\infty}A_k\sum_{i=1}^{\infty}C_{ki}\Phi_i(\xi) \tag{37a}$$

where C_{ki} is given by[13]

$$C_{ki}=\int_0^l(d^2\Phi_k/d\xi^2)\Phi_i d\xi$$
$$=\begin{cases}4(\mu_k\sigma_k-\mu_i\sigma_i)/[(-1)^{i+k}-(\mu_i/\mu_k)^2], & i\neq k\\ \mu_k\sigma_k(2-\mu_k\sigma_k), & i=k\end{cases} \tag{37b}$$

Substituting Eqs. (36) and (37a) in Eq. (35), multiplying with $\Phi_m(\xi)$, and integrating with respect to ξ over the length, one obtains

$$\mu_m^4(A_m+\gamma\omega B_m)-P\sum_{k=1}^{\infty}A_kC_{km}-\omega^2(A_m+\delta_m\eta_0)$$
$$+(8\alpha\omega^2/3\pi)\int_0^l g_s(\xi)[g_s^2+g_c^2]^{1/2}\Phi_m(\xi)d\xi=0$$
$$\mu_m^4(-\gamma\omega A_m+B_m)-P\sum_{k=1}^{\infty}B_kC_{km}-\omega^2B_m$$
$$-(8\alpha\omega^2/3\pi)\int_0^l g_c(\xi)[g_s^2+g_c^2]^{1/2}\Phi_m(\xi)d\xi=0$$
$$m=1,2,\ldots\infty \tag{38}$$

where

$$g_s(\xi)=\sum_{j=1}^{\infty}B_j\Phi_j(\xi)$$
$$g_c(\xi)=\eta_0+\sum_{j=1}^{\infty}A_j\Phi_j(\xi)\quad,\quad\delta_m=2\sigma_m/\mu_m$$

and μ_m are the roots of the equation

$$1+\cosh\mu\cos\mu=0$$

The set of Eqs. (38) can be solved to yield A_m and B_m. In the actual computation the series were truncated to first 4 modes.

III. Experimental Set-up

To assess validity of the analytical approach and to generate relevant design information, an experimental program was undertaken. The tests were performed in a 6′ ×3′ ×4′ rectangular water tank (Fig. 2) constructed from waterproof plywood with front plexiglas panel to help photographing of the deflected model. The tank was equipped with a moveable head to support the tube centrally. A compressed air bottle pressurized an intermediate water tank which was then used to inflate the tube after the test tank had been filled with water. A pressure gauge in the interconnecting piping indicated the inflation pressure. A system of trolley enabled loading of the tube at any desired station. For dynamic testing, the mounting block supporting the model was made a part of the scotch yoke mechanism driven by a 3/16 horsepower d.c. motor equipped with a variable speed control unit.

A set of 10 models made from thin films of polyethylene was tested to cover a wide range of L/d_f ratio, an important system parameter. One end of each tube was sealed by inserting a thin plexiglas plug of the same diameter as the tube and bonding it with epoxy. Each tube was divided into 4 in. sections at which the deflections were measured.

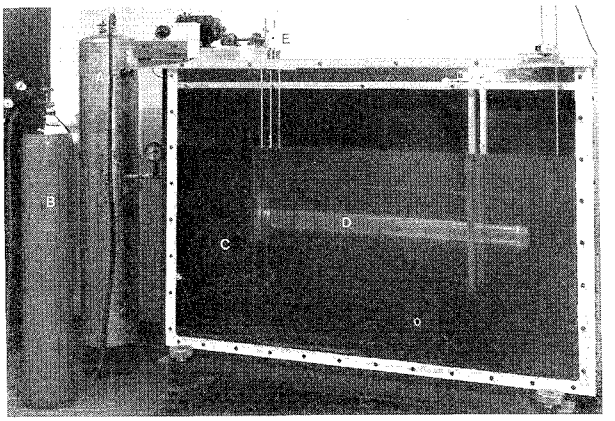

Fig. 2 Experimental setpup: A. water bottle; B. compressed air bottle; C. water tank; D. test model; E. shaking mechanism.

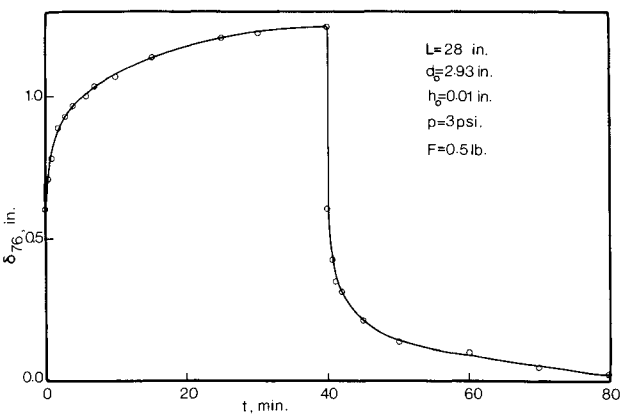

Fig. 3 A typical deflection history for a point on the beam during a loading-unloading cycle.

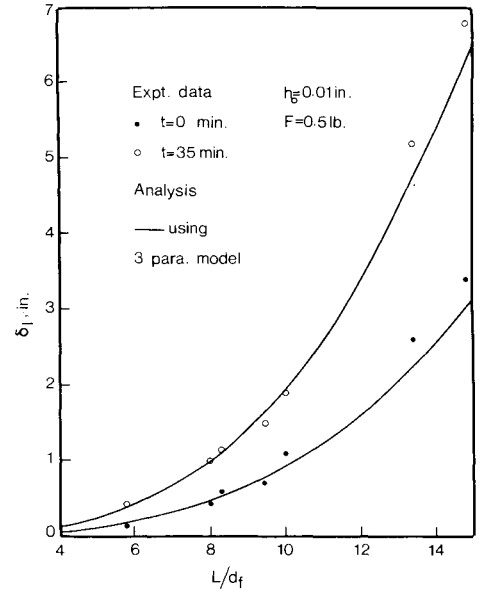

Fig. 4 Tip deflection as a function of L/d_f.

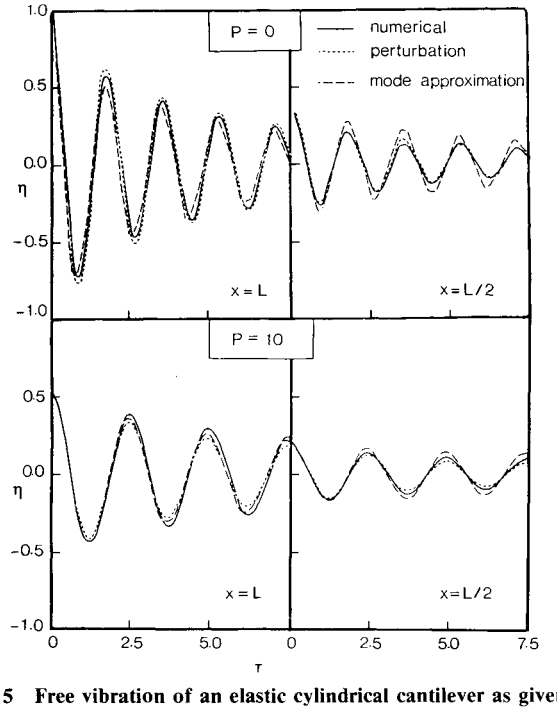

Fig. 5 Free vibration of an elastic cylindrical cantilever as given by approximate and numerical methods.

Since the static deflections are time varying and the measurements at different stations have to be taken at the same instant, photographic technique was applied to record time history of a beam undergoing creeping deformation. 35 mm pictures were taken, initially 30 sec apart with the interval gradually increasing to 5 min as the creep rate diminished. A thin wire strung above the tube served as a reference during these measurements. 16 mm movies were taken for the dynamic tests. The deflection data were analyzed by projecting the pictures on a screen.

IV. Results and Discussion

Although the amount of experimental information generated is rather extensive only a few of the typical results, helpful in establishing trends and deriving conclusions are presented here. Figure 3 shows a typical deflection history during a loading/unloading cycle. It corresponds to a cantilever of 28″ length, 2.93″ diam, 0.010″ wall thickness, and loaded at station 6. The internal pressure is 3 psi. An instantaneous deflection followed by creep is apparent. The creep gradually decreases and becomes almost negligible after about 40 min. With removal of the load, there is an instantaneous drop in the deflection, of the magnitude equal to the instantaneous initial deflection. The model asymptotically returns to the original position following essentially the same behavior as that observed during the load cycle.

The tip deflections at $t=0$ and $t=35$ min are plotted as a function of L/d_f in Fig. 4 for the structural models having a wall thickness of 0.010″ and tip load of 1/2 lb. The lines represent the analytical results as given by Eq. (18) while the isolated points indicate the test data. Potential of the analytical approach becomes apparent as it is able to predict with accuracy even large deflections. Physically this suggests that the curvature can be represented by d^2w/dx^2 without much error even though the deflections are large. The 3 parameter solid does not predict the longtime deformation very well, but a creep compliance of the form

$$J(t) = (0.22 + 0.14t^{0.27}) \times 10^{-4} \tag{39}$$

t in minutes, obtained by fitting a curve to the $J(t)$ given by Lifshitz and Kolsky[14] improves the correlation considerably. It must be recognized that long time strain (say after a few hours) for high stress level has a nonlinear relation with the stress. Findley and Khosla[15] have found the creep of polyethylene to follow the equation

$$\epsilon = \epsilon_0' \sinh(\sigma/\sigma_e) + m' \sinh(\sigma/\sigma_m) t^n \tag{40}$$

where ϵ_0', m', n, σ_e, and σ_m are material constants. On the other hand, Kalinnikov[16] observed the creep relation for polyethyleneterephthalate (mylar) to be of the form

$$\epsilon = \epsilon_0 + a\sigma^m t^n$$

where a, m, n are constants. A similar equation can also be used for polyethylene. But in the study of dynamics of these structures only the short time creep is of significance, since the period of most of the neutrally buoyant structures is very small (a few seconds).

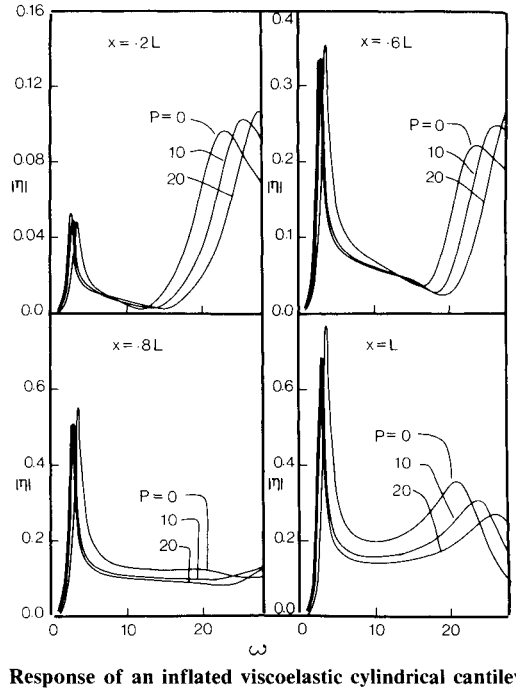

Fig. 6 Response of an inflated viscoelastic cylindrical cantilever to the surface wave excitation.

Table 1 Comparison between analytically and experimentally obtained frequencies

d, in.	L, in.	h, in.	$\omega_{expt.}$, rad/sec.	$\omega_{anal.}$, rad/sec
1.0	12	0.005	16.8	17.8
2.37	19	0.01	15.9	15.5
2.93	44	0.01	4.12	3.20
3.80	40	0.01	4.7	4.44
4.76	40	0.01	5.5	5.20

Figure 5 compares the decay in amplitude due to the hydrodynamic drag as given by the mode approximation, perturbation, and numerical solutions. the initial conditions correspond to the first mode shape i.e. $A(\xi,0) = 0.5\Psi_1(\xi)$. The close agreement between the approximate solution and the numerical method is encouraging.

Figure 6 is a typical plot showing the variation of the amplitude at 4 different points along the length with forcing frequency and pressure parameter. The peaks correspond to the resonance. As expected, as P is increased, the 1st peak occurs for smaller ω, while the 2nd peak moves to a larger value.

The forcing frequencies at which resonance occurs, have been measured for a set of test cylinders. Table 1 compares these with the theoretical predictions. Considering a degree of uncertainty introduced by the added inertia coefficient and elastic properties, the agreement may be considered satisfactory.

V. Conclusions

The important conclusions based on the analysis are summarized as follows: a) The static analysis suggests that a 3 parameter solid model can yield results of sufficient accuracy to be useful in any engineering design of a neutrally buoyant inflatable structure. For the long time creep, a modified creep compliance may be used to improve correlation. b) During the free vibration of an inflated elastic cantilever with hydrodynamic drag and a follower force, the governing equation can be suitably nondimensionalized to render the damping parameter independent of geometrical dimensions of the beam. The results of mode approximation and second-order perturbation analysis compare well with the numerical and the experimental data. c) Dynamical response of the viscoelastic beam to surface wave excitation accounting for the hydrodynamic drag and internal pressure induced follower force, should prove useful in the design of an underwater submarine detection system.

References

[1] Leonard, R. W., Brooks, G. W., and McComb, H. G. Jr., "Structural Considerations of Inflatable Reentry Vehicles," NASA TN D-457, Sept. 1960.

[2] Stein, M. and Hedgepeth, M. M., "Analysis of Partly Wrinkled Membranes," NASA TN D-813, July 1961.

[3] Comer, R. L. and Levy, S., "Deflections of an Inflated Circular Cylindrical Cantilever Beam," *AIAA Journal*, Vol. 1, July 1963, pp. 1652-1655.

[4] Topping, A. D., "Shear Deflections and Buckling Characteristics of Inflated Members," *Journal of Aircraft*, Vol. 1, Sept.-Oct. 1964, pp. 289-292.

[5] Douglas, W. J., "Bending Stiffness of an Inflated Cylindrical Cantilever Beam," *AIAA Journal*, Vol. 7, July 1969, pp. 1248-1253.

[6] Landweber, L., "Vibration in an Incompressible Fluid," Iowa Institute of Hydraulic Research, Rept., Contract Nonr. 3271 (01) (x), May 1963.

[7] Landweber, L., "Vibration of a Flexible Cylinder in a Fluid," *Journal of Ship Research*, Vol. 11, Sept. 1967, pp. 143-150.

[8] Warnock, R. G., "Added Masses of Vibrating Elastic Bodies," Iowa Institute of Hydraulic Research, Rept., Contract Nonr. 3271 (01) (x), Feb. 1964.

[9] Douglas, W. J., "Natural Vibrations of Finitely Deformable Structures," *AIAA Journal*, Vol. 5, Dec. 1967, pp. 2248-2253.

[10] Keulegan, G. H. and Carpenter, L. H., "Forces on Cylinders and Plates in an Oscillating Fluid," *Journal of Research of the National Bureau of Standards*, Vol. 60, May 1958, pp. 423-439.

[11] Anderson, J. M. and King, W. W., "Vibration of a Cantilever Subjected to a Tensile Follower Force," *AIAA Journal*, Vol. 7, April 1969, pp. 741-742.

[12] Cunningham, W. J., *Introduction to Nonlinear Analysis*, McGraw-Hill, New York, 1958, pp. 135-137.

[13] Paidoussis, M. P., "Dynamics of Flexible Slender Cylinders in Axial Flow," *Journal of Fluid Mechanics*, Vol. 26, Pt. 4, Dec. 1966, pp. 717-736.

[14] Lifshitz, J. M. and Kolsky, H., "Nonlinear Viscoelastic Behaviour of Polyethylene," *International Journal of Solids and Structures*, Vol. 3, May 1967, pp. 383-397.

[15] Findley, W. N. and Khosla, G., "An Equation for Tension Creep of Three Unfilled Thermoplastics," *Society of Plastic Engineers Journal*, Vol. 12, Dec. 1956, pp. 20-25.

[16] Kalinnikov, A. E., "Creep and Aftereffect of PET Films Under Conditions of Uniaxial Stress," *Mekhanika Polimerov*, Vol. 1, No. 2, Mar. 1965, pp. 59-63.